Measuring phonons in protein crystals

Gheorghe Acbas[a], Katherine A. Niessen[a], Deepu K. George[a], Edward Snell[b,c] and A.G.Markelz[a]*
[a]Department of Physics, University at Buffalo, SUNY, Buffalo, New York, USA
[b]Department of Structural Biology, University at Buffalo, SUNY, Buffalo, New York, USA 14260-1500; [c]Hauptman Woodward Medical Research Institute, Buffalo, New York, USA 14203-1102

ABSTRACT

Using Terahertz near field microscopy we find orientation dependent narrow band absorption features for lysozyme crystals. Here we discuss identification of protein collective modes associated with the observed features. Using normal mode calculations we find good agreement with several of the measured features, suggesting that the modes arise from internal molecular motions and not crystal phonons. Such internal modes have been associated with protein function.

Keywords: protein dynamics, correlated motions, molecular vibrations, terahertz spectroscopy, phonons, molecular crystals, normal modes

1. INTRODUCTION

Correlated motions in proteins have long been predicted to lay in the terahertz frequency range (*1*). Unfortunately the measurement of these modes has been problematic due to overlap with the broadband response of biological water and possible librational motions of surface side chains. Polarization difference spectroscopy is a method that can be used to suppress a homogeneous background from orientation sensitive resonances, however the size for typical protein crystals is far below the diffraction limit at terahertz frequencies. Recently great advances in THz near field microscopy have been made(*2*). Recently we have demonstrated narrow band orientation sensitive absorption features for protein crystals using terahertz near field microscopy.

We use a THz time domain near field microscope method based on that by Planken (*2*). A challenge in measuring the absorbance is proper referencing and removal of etalon. We address both the referencing and etalon concerns by self-referencing. As we are interested in the change in absorbance with orientation, we use a single orientation of the crystal as our reference and calculate a difference absorbance using the following:

$$\begin{aligned}\Delta Abs &= -2\ln\left[\frac{|E_t(\omega,\theta)|}{|E_t(\omega,\theta_{ref})|}\right] \\ &= -2\ln\frac{F(\omega)|E_i(\omega)|e^{-\alpha(\omega,\theta)d/2}}{F(\omega)|E_i(\omega)|e^{-\alpha(\omega,\theta_{ref})d/2}} \\ &= \left[\alpha(\omega,\theta)-\alpha(\omega,\theta_{ref})\right]d\end{aligned} \quad (1)$$

Where $|E_t(\omega,\theta)|$($|E_i(\omega,\theta)|$) is the magnitude of the transmitted (incident) electric field, $\alpha(\omega,\theta)$ is the sample's absorption at orientation angle θ, and d is the sample thickness. $F(\omega)$ is the frequency dependent transmission due to Fresnel loss at interfaces, waveguide transmission for the aperture, and etalon effects. This factor should be orientation independent.

In Figure 1 we show the image plot of the orientation and frequency dependence measured for a hydrated lysozyme crystal. As seen there are several strong orientation sensitive features, highlighted by dashed lines. The 180° symmetry cannot arise from any artifact within the measurement and must arise from the sample itself. These features arise from intramolecular vibrations. As a starting point for these measurements we assume that the crystal contact forces are very weak, then we can calculate the net crystal response by summing the single molecule response over the unit cell, accounting for the molecular rotations for the crystal symmetry group:

Ultrafast Phenomena and Nanophotonics XVII, edited by Markus Betz, Abdulhakem Y. Elezzabi, Jin-Joo Song, Kong-Thon Tsen, Proc. of SPIE Vol. 8623, 862305 · © 2013 SPIE · CCC code: 0277-786X/13/$18
doi: 10.1117/12.2006275

$$Abs_{xtal} = \sum_{\substack{j=xtal \\ rotation \\ matrices}} \sum_{i=7}^{3N} \frac{\gamma^2 / \omega_i}{(\omega - \omega_i)^2 + \gamma^2} \left[\left(\overrightarrow{R_j} \frac{\partial \vec{p}}{\partial q_i} \right) \hat{\lambda} \right]^2 + Abs_{isotropic} \qquad (2)$$

where $\partial \vec{p} / \partial q_i$, ω_i, γ_i, $\hat{\lambda}$, and $\overrightarrow{R_i}$ are the dipole derivative, mode frequency, linewidth, light polarization unit vector, and rotation matrix associated with the crystal symmetry respectively. For the initial comparison of the measured and calculated response we used Version 32 of CHARMM (*3*). The x-ray structure file 1bwh.pdb was used as the starting structure. The 92 crystal waters are included using TIP3 (TIP3p) explicit solvent. The energy minimized structure was then used for Normal Mode Analysis (NMA), which determines the eigenfrequencies, eigenvectors and net dipole derivative for each vibrational mode. The spectra are calculated assuming a single linewidth $\gamma_i = \gamma = 5$ cm^{-1} linewidth for all modes. We calculate the expected anisotropic response using Eq. (2) for the polarization rotated perpendicular to (110), the incident crystal face used for the measurements. The measured signal is proportional to the difference in absorbance for different orientations relative to a reference orientation. The THz polarization along (001) is used as the reference orientation, giving:

$$\Delta Abs_{xtal}(\hat{\lambda}, \hat{\lambda}_{ref}) = Abs_{xtal}(\hat{\lambda}) - Abs_{xtal}(\hat{\lambda}_{ref}) \qquad (3)$$

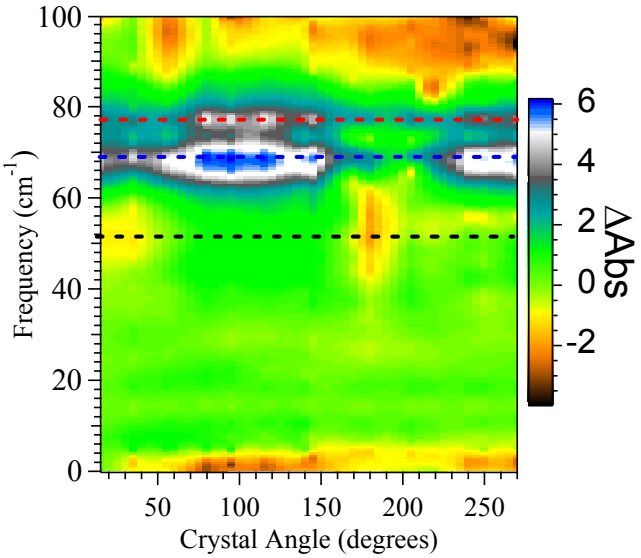

Figure 1. Measured ΔAbs for a hydrated tetragonal lysozyme crystal as a function of orientation angle and frequency. The THz is incident on the (110) face.

2. RESULTS

In Fig. 2 we show the frequency and orientation dependence of the calculated Dabs. The two high frequency features seen in the measurements are immediately apparent. The scaling of the image plot obscures the additional agreement with the 51 cm^{-1} feature, which can be more clearly seen in Figure 3, which shows a waterfall plot of the calculated ΔAbs. spectra.

In Fig. 3 we show the displacement vector diagrams for the modes corresponding to the features seen in the measurements. The displacement vectors are drawn from the α carbons and their lengths are proportional to the atomic displacement for the net eigenvector. The motion corresponds to all atoms moving in a concerted fashion along these vectors. The lowest frequency mode, observed at 51 cm^{-1} and calculated at 47 cm^{-1} consists of relative motion between helices and compressive motion in the binding site. The higher frequency mode observed at 69 cm^{-1} and calculated at 67 cm^{-1} also has some motion between helices and at the binding site, but somewhat lower amplitude. The highest

frequency feature observed at 78 cm^{-1} and calculated at 80 cm^{-1} has little motion near the binding site and large amplitude motion at the ends of the protein. It has long been speculated that these correlated motions, while at ps time scale, contribute to protein conformational dynamics and alteration of the motions can effect function. Calculations show that functional conformational change in many biomolecular systems can be simulated using only the first few collective vibrational modes of the system (*4, 5*).

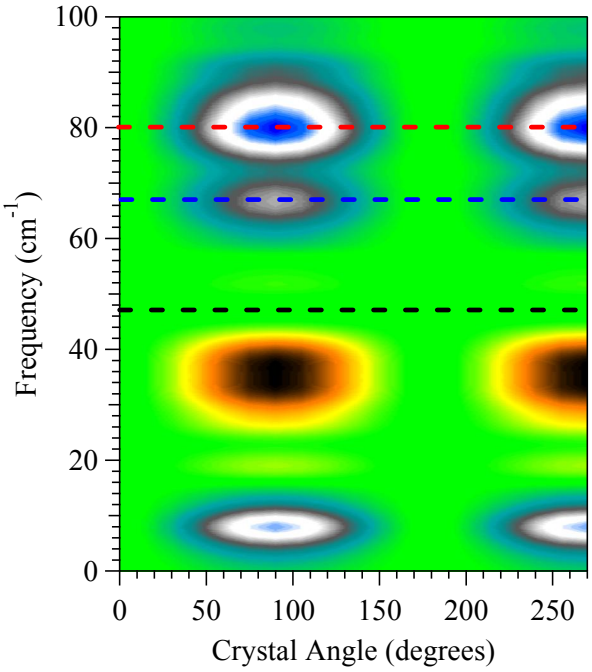

Figure 2. Calculated ΔAbs for a tetragonal lysozyme crystal is shown as a function of orientation angle and frequency. Several features consistent with the frequency dependent and orientation dependence are seen in the measurement.

3. CONCLUSIONS

Orientation dependent sharp absorbances are observed for protein crystals using near field THz microscopy. The absorbances are likely related to correlated motions within the protein and may have functional relevance.

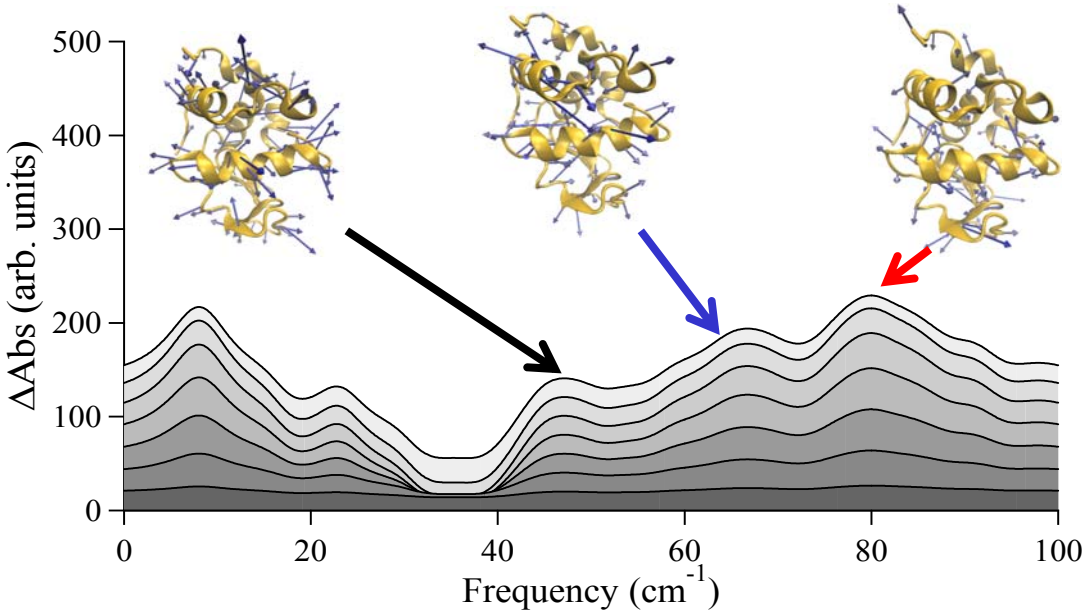

Figure 3.Calculated Δabs spectra for different rotations with the vector diagrams of the modes corresponding to the peaks in the difference spectra observed in measurements.

ACKNOWLEDGMENT

We thank the National Science Foundation MRI^2 grant DBI2959989 for support.

REFERENCES

1. Brooks, B., and Karplus, M. (1985) Normal modes for specific motions of macromolecules: Application to the hinge bending mode of lysozyme, *Proc. Natl. Acad. Sci. U. S. A. 82*, 4995-4999.
2. Planken, P. C. M. (2011) Introduction to the Special Issue on "Terahertz Near-field Optics", *Journal of Infrared Millimeter and Terahertz Waves 32*, 975-975.
3. Brooks, B. R., Bruccoleri, R. E., Olafson, B. D., States, D. J., Swaminathan, S., and Karplus, M. (1983) CHARMM: a program for macromolecular energy, minimization, and dynamics calculations, *J. Comput. Chem. 4*, 187-217.
4. Karplus, M., and Kuriyan, J. (2005) Molecular dynamics and protein function, *Proc. Natl. Acad. Sci. U. S. A. 102*, 6679-6685.
5. Bahar, I., and Rader, A. J. (2005) Coarse-grained normal mode analysis in structural biology, *Curr. Opin. Struct. Biol. 15*, 586–592.